

Raman spectroscopy for strain measurement in state-of-the-art LSI

Atsushi Ogura¹, Daisuke Kosemura¹, Munehisa Takei^{1,2}, and Motohiro Tomita^{1,2}

¹School of Science and Technology, Meiji University, 1-1-1 Higashimita, Tama-ku, Kawasaki, 214-8571, Japan
Phone/Fax: +81-44-934-7324, E-mail: a_ogura@isc.meiji.ac.jp

²JSPS Research Fellow

1. Introduction

Strained-Si is one of the most promising technologies in modern high-performance MOSFETs. The strain contribution for the performance improvement has increased with the progress of MOSFETs scaling. It is indispensable to control the strain variations in each MOSFET, which is directly correlated to the device performance. Raman spectroscopy can non-destructively evaluate the stress sensitively with relatively high spatial resolution ($<1\ \mu\text{m}$) [1]. Moreover, the evaluation depth can be controlled by selecting appropriate wavelength of the incident laser. The extremely surface sensitive analysis ($<5\ \text{nm}$), which corresponds to the MOSFET channel, can be achieved by using ultra-violet (UV) excitation [2]. However, the spatial resolution in the Raman spectroscopy has not been satisfactory for state-of-the-art LSI which has been extremely scaled down in recent years. Moreover, the multi-axis strain evaluation by Raman spectroscopy has been difficult, thus hardly been performed especially for (100)Si. We have improved spatial resolution in Raman measurement by adopting a quasi-line excitation source [2] and high-numerical aperture (NA) objective lens. Additionally, we applied the Super-resolution technique [3] and peak-separation methods, and succeeded in the strain evaluation for fine-structure ($\sim 30\ \text{nm}$). We also clarified that high-NA objective lens could generate the Z-polarization light. TO-phonon mode in Si(100), which was not observed conventionally by the Raman selection-rule, could be excited by this light, and we succeeded two-axis strain evaluation [4].

In this paper, we report the strain evaluation for state-of-the-art LSI by various sophisticated Raman spectroscopy.

2. Experiment

We prepared several samples for strain measurements. Sample-A was line-and-space pattern of tensile SiN film on Si substrate. Sample-B was gate-last pMOSFET with eSiGe and a compressive stress linear after the dummy gate removal process, thus the channel region was exposed. Sample-C was commercially available 32nm-node-MPU (clock frequency was 3.33 GHz). Wiring and gate electrodes were removed to perform Raman measurement. Two-axis strain evaluation was performed for SSOI (strained-Si on insulator) substrate with and without patterning (Sample-D).

The strain measurements were performed by Raman spectroscopy equipped with a quasi-line excitation source of a visible ($\lambda = 532\ \text{nm}$) and a UV ($\lambda = 363.8\ \text{nm}$) laser [2]. The excitation source light is focused on the sample by the dry (NA = 0.5) or oil immersion (NA = 1.4) objective lens.

3. SiN film line and space pattern

Figure 1 shows the strain profiles across the various spaces in the 80nm-thick-tensile SiN film line-and-space pattern (sample-A). The compressive strain was induced in SiN film edges, while the tensile strain was induced in the space region. The tensile strains in the space edges were larger than that in the space center. The tensile strain in the

space region was increased with decreasing the space width (size-effect). However, the U-shape strain profile in the space region was disappeared less than $1\ \mu\text{m}$ space width and the size effect could not be observed less than $0.5\ \mu\text{m}$ due to the lack of the spatial resolution.

4. Gate-last pMOSFET after dummy gate removal

Figure 2 shows (a)two- and (b)one-dimensional strain profiles in the channel region for sample-B. From these figures, the strains at the channel edges were larger than those at the channel centers. The size effect was observed in the real MOSFET as well as SiN pattern. Furthermore, we also observed U-shape strain profile in Wgate direction.

Figure 3 shows the compressive strain in the channel center extracted from the strain profile like Fig. 2 depending on Lgate. The strain values of Lgates less than $0.26\ \mu\text{m}$ were obtained by long-exposure measurement and the peak separation methods. Red, blue and green lines were strains for pMOSFET with/without eSiGe and simulation results, respectively. The strain incassation by size effect could be observed even in $30\ \text{nm}$. eSiGe was effective for the strain introduction especially for the Lgate less than $0.1\ \mu\text{m}$. Finally, we clarified that the huge compressive stress of $-2.5\ \text{GPa}$ was induced in the $30\ \text{nm}$ Lgate. These results were good agreement with the simulation.

5. Commercially available 32nm-node-MPU

Figure 4 (a) shows TEM images of 32nm-node-MPU after the channel exposure. Figure 4 (b) and (c) were Raman spectra obtained from pMOSFET and nMOSFET, respectively. The dashed lines were fitting results which is deconvolution to the peaks from Si-sub. and strained-Si channel. The strained-Si peak in the pMOSFETs (Fig. 4(b)) shifted toward higher frequency side of approximately $7.5\ \text{cm}^{-1}$ which corresponds to $-3.75\ \text{GPa}$ (compressive) with the assumption of the uni-axial stress along the channel direction. On the other hand, the strained-Si peak in the nMOSFETs (Fig. 4(c)) was $-1.7\ \text{cm}^{-1}$ corresponding to $0.85\ \text{GPa}$ (tensile).

6. Two-axis strain evaluation for SSOI

Figure 5 shows two-axis strain evaluation for SSOI (sample-D). Raman spectra denoted by the red and blue lines were taken under the LO- and TO-active conditions, respectively. TO and LO modes are expected to be degenerated in strained Si. TO mode was shifted toward higher frequency side than LO mode. Thus, we succeeded the excitation of both TO and LO mode independently. Thus, two-axis strain analysis became possible using Z-polar component of the incident light thanks to the high NA oil immersion objective lens.

Figure 6 (a) shows the schematic diagram of patterned SSOI. Figure 6 (b) and (c) were two-axis strains and the strain relaxation ratios. The SSOI length was varied from $5000\ \text{nm}$ to $400\ \text{nm}$ while SSOI width was set at $200\ \text{nm}$. Open circle and triangle were stress along SSOI length and width, respectively. Red and blue lines were FEM stress simulation along SSOI length and width, respectively. The

stress along the SSOI length was relaxed with reducing the SSOI length. On the other hand, the stress along the SSOI width was almost constant. It was clear that the stress along the SSOI length was sensitive to the SSOI length, and the relaxation ratio was larger than the stress along the SSOI width. The stress relaxation trends were good agreement with FEM simulation.

7. Conclusions

The strain analyses were performed for patterned SiN film, gate-last pMOSFET, 32nm-node-MPU and SSOI. We clarified the mechanism of the strain introduction in the MOSFET and observed huge strain induced in state-of-the-art LSI. Moreover, we proposed multi-axis strain evaluation technique using high-NA objective lens. We believe it is indispensable to control the strain based on the detailed analysis and consideration to realize the high-performance LSI.

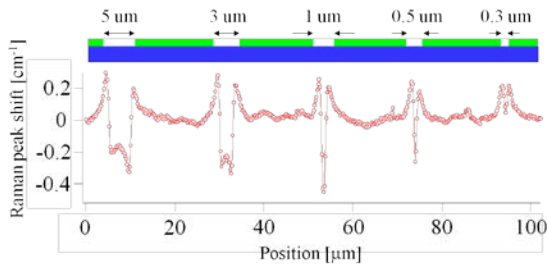


Fig. 1 (a) Strain profiles obtained from line-and-space pattern tensile SiN film (80nm-thick) on Si with various space width.

Acknowledgement

The authors would like to appreciate Dr. S. Mayuzumi and Dr. H. Wakabayashi for their fruitful discussion. Part of this study was supported by STARC.

References

- [1] I. De Wolf *et al.*, J. Appl. Phys., **79**, 7148 (1996).
- [2] A. Ogura *et al.*, Jpn. J. Appl. Phys., **45**, 3007 (2006).
- [3] M. Tomita *et al.*, Jpn. J. Appl. Phys., **50**, 010111 (2011).
- [4] D. Kosemura *et al.*, Appl. Phys. Lett. **96**, pp.212106-1 (2010).

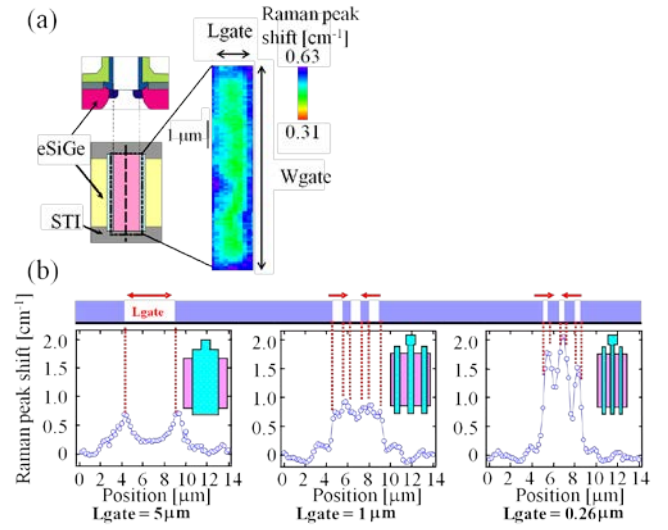


Fig. 2 (a)Two- and (b)one-dimensional strain profiles across channel direction obtained from gate last pMOSFET after dummy-gate removal process.

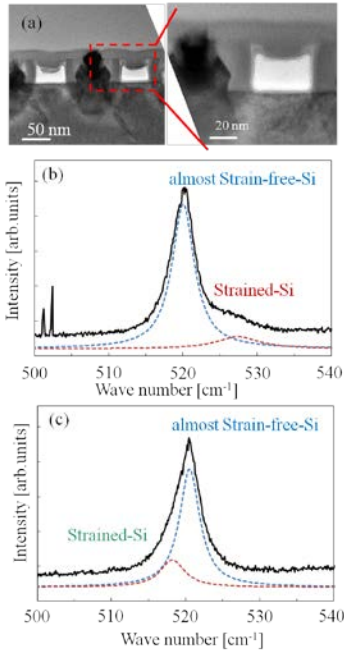


Fig. 4 (a) TEM images of 32nm-node-MPU after the channel exposure. Raman spectra obtained from (b)pMOSFET and (c)nMOSFET, respectively.

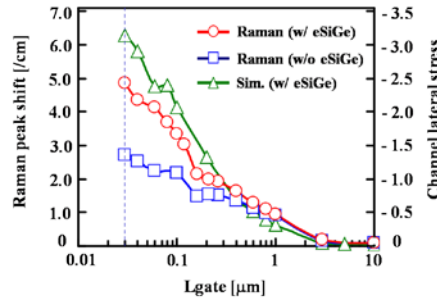


Fig. 3 Strains in channel obtained from sample-B dependence on Lgate. Red, blue and green lines were Raman results for pMOSFET with/without eSiGe and stress simulation, respectively.

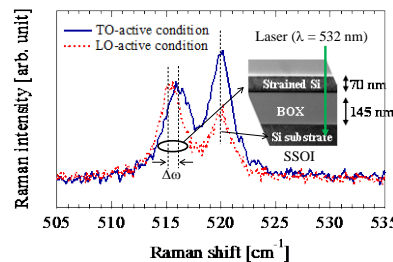


Fig. 5 Raman spectra taken under TO and LO active conditions from SSOI.

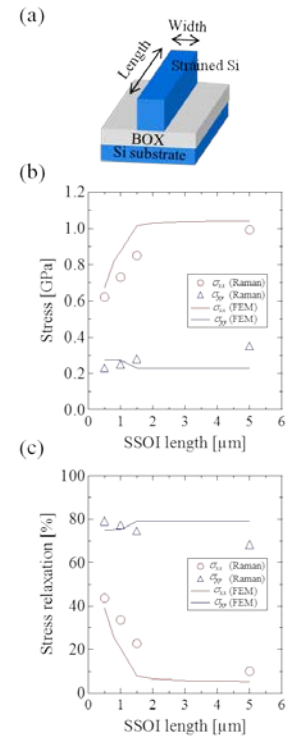


Fig. 6 Two-axis strain evaluation for patterned SSOI. Open circle and triangle were stress along length and width, respectively. Lines were FEM stress simulation.